Progress In Electromagnetics Research C, Vol. 96, 73–85, 2019

Trident Shape Ultra-Large Band Fractal Slot EBG Antenna for Multipurpose IoT Applications

Pankaj K. Goswami[1, *] and Garima Goswami[2]

Abstract—Wireless technology has significant improvement in features enhancement of device applications. It is highly desirable to operate multiple applications from a single device. A compact size antenna is presented for a variety of IoT based applications, such as home automation, surveillance, satellite communication, vehicle tracking, and medical instruments. This article explores an analytical solution of ultra-large band frequency characteristics of a compact size, trident shape, fractal patch antenna. The overall structure has dimension $18 \times 12 \times 1.6\,\text{mm}^3$. This antenna exhibits the multi-edge radiating effects of fractal structure with the help of ground optimization technique. The design evolution consists of a performance measure of the antenna with varying characteristics of the EBG patterns with respect to fractal structure. The design is validated by fabricating the antenna on an FR4 (4.2) substrate, and the return loss & radiation characteristics are measured. The measured $|S_{11}|$ has the impedance bandwidth of 1.59–13.31 GHz and sustainable radiation characteristics. This miniaturized antenna is compatible with the GSM, GPS, Bluetooth, Wi-Fi, WLAN, Wi-MAX, ISM, and other UWB spectrums. The gain of the antenna is 2.52 dBi for the complete operating range. Therefore, the proposed antenna is highly compatible with various wireless devices associated with IoT applications.

1. INTRODUCTION

1.1. Wireless IoT Based Applications

The multiple operations from IoT enabled devices require an antenna with ultra-large band characteristics. This antenna allows devices to communicate with each other in multiple frequency-dependent applications. Wireless Personal Area Network (WPAN) is an emergent application of such devices. A simple block diagram of a few such applications is illustrated in Figure 1.

Dual-band features are observed in planer antennas by defected ground structure (DGS), slot, fractal, split rings, etc. [1, 2]. Multi-layered and multi-patch structures are also preferred to obtain ultra-wideband (UWB) characteristics [3, 4]. The effective utilization of a tapered slot antenna with tuning stub is marked for complete coverage of UWB frequency [5]. Extensive applications of UWB antenna are found in the smart home system. Multiple IoT based devices can be connected together using a common platform for controlling and signalling purpose. The smart devices' intra-connectivity and interconnectivity on the web or mobile handset require broadband internet connections. Smart home and smart industries are the extensive application areas of IoT based devices [6–8]. The dependence of these IoT devices relies on wireless communications and crucially on antenna structure. The antenna position and profile affect signal fading and propagation. Therefore, this requires an integration of generated field frequency in multiple bands, processed by an antenna in smart devices [9, 10]. Table 1 shows various wireless applications with respect to allotted frequency range as per FCC standards [11].

Received 30 July 2019, Accepted 17 September 2019, Scheduled 25 September 2019

* Corresponding author: Pankaj Kumar Goswami (g.pankaj1@gmail.com).

[1] Department of Electronics and Communication Engineering, Teerthanker Mahaveer University, Moradabad 244001, India.

[2] Department of Electrical Engineering, Teerthanker Mahaveer University, Moradabad 244001, India.

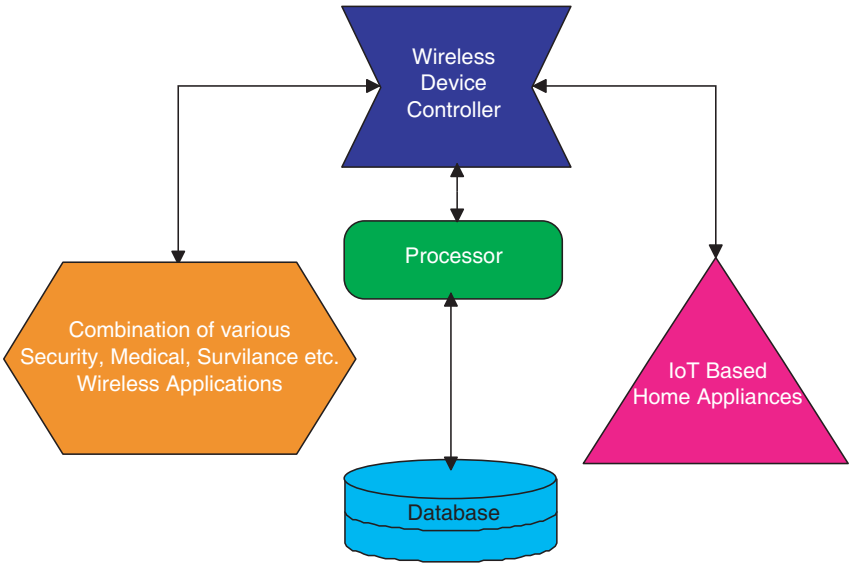

Figure 1. Broadband antenna based IoT applications.

Table 1. Frequency based IoT applications.

IoT based applications	Frequency range
Energy control unit	2.45 GHz & 5.8 GHz
security, motion, surveillance, sensors and camera	5.8 GHz
LED light bulbs	2.45 GHz
HVAC duct dampers	900 MHz
Global Positioning System	1.565–1.585 GHz
	1.227–1.575 GHz
Digital Communication System	1.71–1.88 GHz
Personal Communication System	1.85–1.99 GHz
Universal Mobile Telecommunications System	1.92–2.17 GHz
International Mobile Telecommunications — 2000	1.885–2.200 GHz
Industrial, Scientific and Medical and	2.4–2.484 GHz
Wireless Local Area Network	5.15–5.35 GHz
	5.725–5.825 GHz
Long Term Evolution	2.5–2.69 GHz
Worldwide Interoperability for Microwave Access	2.3–2.7 GHz
	3.4–3.6 GHz
For Blue tooth applications	2.4–2.4835 GHz

1.2. Miniaturized Ultra-Wide Band Antenna

The state of the art in broadband antennas in the effect of truncated ground-plane for UWB applications is described. A scheme, for the design and optimization of wideband printed planar monopoles using a genetic algorithm (GA), different impedance bandwidth enhancing techniques, and a wideband folded-shorted antenna are presented in [12–16]. Design aspects of printed monopole antennas for UWB applications are discussed in [17], and an effective technique is presented for UWB monopole

antenna size reduction with symmetric structure [18]. The effect of single and dual microstrip lines on impedance matching over return loss characteristics of UWB printed antenna is discussed. In [19], working principles of coplanar-waveguide CPW-fed, UWB printed antennas are considered. Adopted integration concept is used for the same printed antenna for narrowband and wideband applications in [20]. UWB monopole antenna with CPW-fed, glass shape printed front side of the substrate can be used as a wideband antenna. On the rear side of the substrate, the narrowband antenna is printed to use the UWB antenna as its ground plane. Bandwidth widening technique of a multilayer patch antenna for X-band applications is proposed in [21]. A method to enhance the bandwidth having two compact antennas with the circular ground and reduced fractal ground is proposed in [22]. A method of enhancing the bandwidth by cutting two new slots on the ground plane is presented in [23]. In this paper, a fractal slotted U-shape patch antenna is presented with ground electromagnetic band gap (EBG) deformation. The utility of the antenna is observed in multipurpose IoT based applications. The versatility of structure is highly useful for real-time wireless applications due to its compact design and ultra-large band characteristics.

2. DESIGN METHOD

A trident-shape fractal antenna is modified from a basic square shape of patch $10 \times 10\,\text{mm}^2$ over a $12 \times 18 \times 16\,\text{mm}^3$ FR4 substrate. At the initial stages, the square patch MSA is modified by cutting slots through its edges as shown in Figure 2. By creating a trident like structure, the antenna has more capacitive reactance at the top edges while the rest of the surface part of the patch exhibits inductive properties. The effective electrical length of the circuit is matched through microstrip lines to the coaxial feed system. At the other side of the patch, the ground is deformed through an iterative process, and EBG structures are introduced for an effective match of equivalent impedance. The EBG structures are used at the lower edge of the ground surface of the antenna in the form of vertical rectangles. These gaps help the reduction of spurious feed radiations. A slot of length 'L_6' and width 'W_3' is cut along both the edges of the patch vertically while a small strip of width 'L_3' is cut vertically in design 1. The parallel LC oscillating circuits resonate into an antenna equivalent circuit. The current distribution has a high current density at the centre of the patch for low operating frequencies while it is low at the edges. Thus, the insertion of slots along the edges makes the antenna shorten in its effective electrical length.

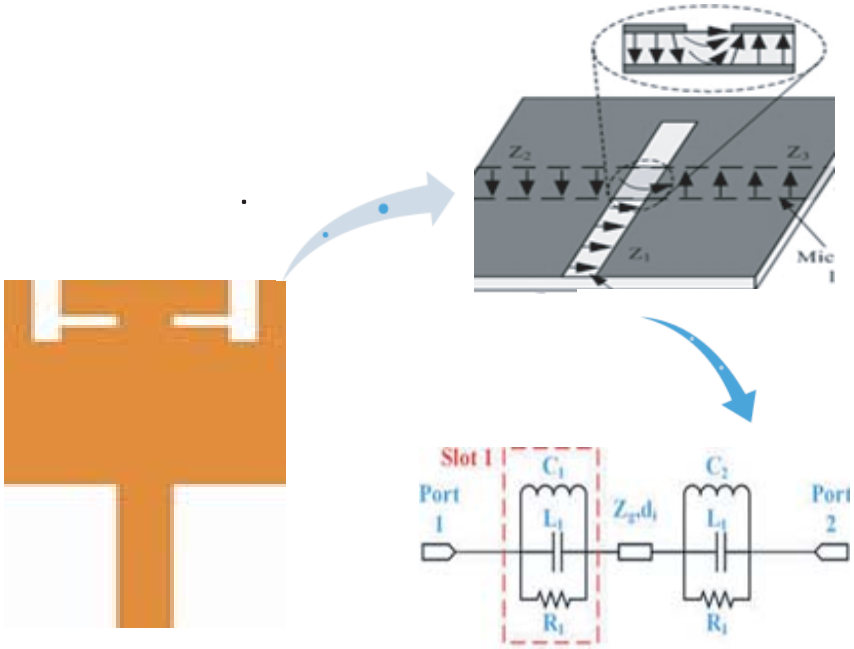

Figure 2. Effect of slot on square patch.

Length of slot is given either quarter wave length or half wave length of centre frequency. The total length L of a slot can be taken as $0.45\lambda_{eff}$-slot.

The various slot lengths and effective iteration through modelling can be obtained by following equations [24].

Distance between slots

$$D = \frac{v_0}{f_{\text{low}}\sqrt{\epsilon_{reff}}} - 2(L + 2\Delta L - w) \tag{1}$$

The Lower operating frequency (f_L) and upper operating frequency (f_H) of U slot design can be approximately determined from

$$f_L = \frac{c}{L_1 + W_1} \quad \text{and} \quad f_H = \frac{c}{L_2 + W_2} \tag{2}$$

L = Length of the patch L_2 = Outer length of U slot
W = Width of the patch W_2 = Outer width of U slot
L_1 = Inner U slot length w = Thickness of the slot
W_1 = Inner length of U slot

Length of the inner slot is taken as $L1 = 0.45\lambda$ or 0.5λ.

The value of ε_{re} is calculated by using the inner U slot width $(L_1 - 2w)$.

If the orientation of U slot is as shown below, the resonant length is calculated by

$$l_u = 2\,(L_2 - w) + W_2 + \left(\frac{0.2l}{\sqrt{\epsilon_{reff}}}\right) \tag{3}$$

Narrow slots are placed close to the radiating edges, where the current is nearly minimum for TM10 mode. The length of the current path is increased due to the slot which leads to additional inductance in series. Hence, wide bandwidth is generated as the resonant circuits become coupled. The slots aggregate the currents, which give additional inductance controlled by the patch width. An alternate way to reduce the resonance frequency of the MSA is to increase the path length of the surface current by cutting slots in the radiating patch. Considering the slot as a half wavelength resonator, slot frequency (f_s) can thus be expressed as

$$f_s = \frac{c}{2L}\sqrt{\frac{2}{\epsilon_r + 1}} \tag{4}$$

Slot length (l) is taken to be equal to a quarter-wave in length, with an additional length (due to the circulation of currents around the shorted end of slot), the effective slot length is given as

$$l_e = l + \left(\frac{0.4l}{\sqrt{\epsilon_{reff}}}\right) \tag{5}$$

Since the surface currents circulate around the slot, the effective dielectric constant (ϵ_{reff}) is calculated by using the average of the widths on either side of the slot. The slot frequency is calculated by

$$f_{\text{calc}} = \frac{c}{4l_e\sqrt{\epsilon_{reff}}} \tag{6}$$

If slot length (l) is taken to be equal to a half-wave in length, with an additional length (due to the circulation of currents around the shorted end of slot), the effective slot length is given as

$$l_e = l + \left(\frac{0.2l}{\sqrt{\epsilon_{reff}}}\right) \tag{7}$$

From the above discussions, the antenna evolutions are represented in Figure 3. The simplified trident structure is repeated using fractal shape geometry, and the final proposed structure is obtained as Figure 4. Therefore, the proposed model is the combination of the effects of the slotted geometry in trident shape and repetitions of fractal geometry. The additional design modification is obtained by DGS and vertical EBG pattern in the ground plane. These patterns enable antennas to operate at comparatively low edge frequency and provide better impedance bandwidth within the same structure.

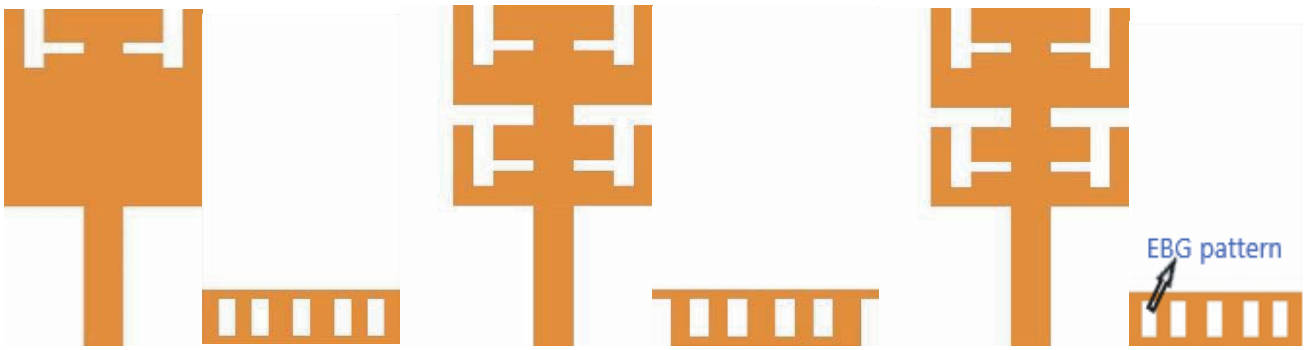

Figure 3. Design evolution, (a) trident structure with EBG, (b) fractal slots trident with modified EBG, (c) fractal slots trident with optimized EBG.

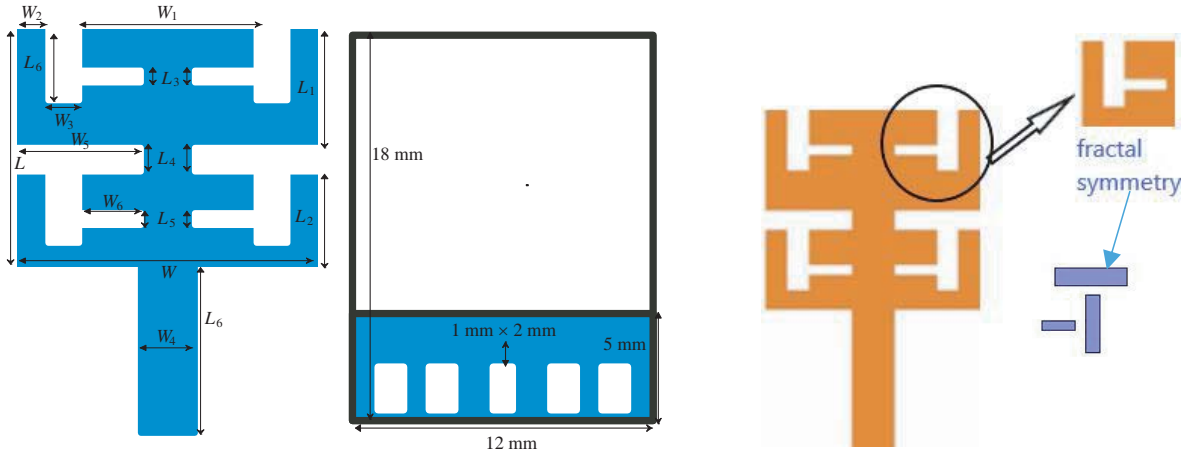

Figure 4. (a) Antenna design and (b) fractal symmetry.

The simple rectangular band gaps with little alteration in pattern is shown in Figures 3(a), (b), and (c). This design evolution has been modelled & analysed on high-frequency structure simulator.

The prototype of antenna fabricated on commercially available FR4 materials with dielectric constant 4.4 and loss tangent 0.002. The antenna is experimented and validated for the previously discussed IoT based application. The desired antenna model is simulated through multiple design iterations. The first antenna design has only one part of trident geometry and is associated with the deformed ground structure. This ground also exhibits vertical slots of EBG patterns that helps in broadening of impedance bandwidth. Further, the design is rectified using two-fold fractal symmetry on the modified ground structure. The cutting edges of the ground are created to suppress the scattering of low frequency from the edges. Any further modification in the geometry causes degenerative suppression of electric field. The proposed antenna is shown in Figure 4 with patch and optimized ground geometry. An equivalent diagram of the upper patch layer is depicted in Figure 5(a). Each unit of slot design makes a parallel resonance circuit, and all are connected in series with the complete inductive surface of the patch.

This resonating unit makes net antenna impedance matched for a wider band of operations. On the other hand, the repeated cell of EBG equivalent circuits enables the antenna to resonate, even at the lower corner of the frequencies for the same physical structure shown in Figure 5(b). Various dimensions of the proposed model are shown in Table 2. The antenna prototype is designed on commercially

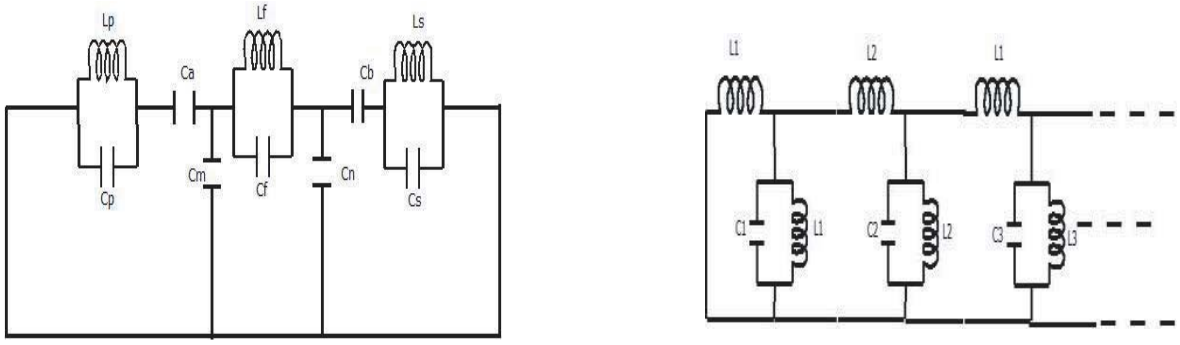

(a) (b)

Figure 5. Equivalent diagram, (a) capacitive slot loading, (b) ground EBG structure.

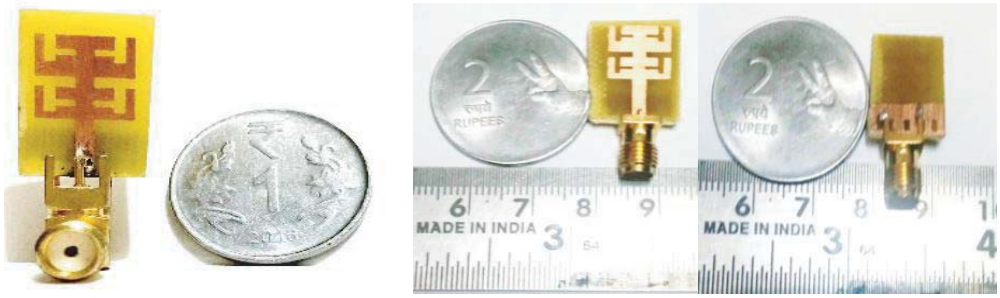

Figure 6. Antenna prototype.

Table 2. Design measurements.

parameter	(mm)	parameter	(mm)
L	10	W	10
L_1	5	W_1	6
L_2	4	W_2	1
L_3	0.5	W_3	1
L_4	1	W_4	2
L_5	0.5	W_5	4
L_6	3	W_6	2

available FR4 materials of thickness 1.6 mm and dielectric constant 4.2. The structure is realized on a $12 \times 18\,\text{mm}^2$ substrate as shown in Figure 6.

3. RESULTS AND DISCUSSION

The antenna is modelled and simulated by High-Frequency Structure Simulator. This trident-shape fractal antenna is designed to obtain UWB and GSM/GPS/Bluetooth operations. Many IoT based applications are compatible with the operating frequency range of proposed antenna. Multiple iterations are executed, and simulation results are shown in Figure 7. The first modification of the antenna is obtained from the basic square patch of $10 \times 10\,\text{mm}^2$, and it is found radiating in the lower range of UWB due to the capacitive loading on the top of the patch and optimized DGS. The further improvement in the patch geometry is the repetition of the trident structure. This leads to the effect of fractal structure. The

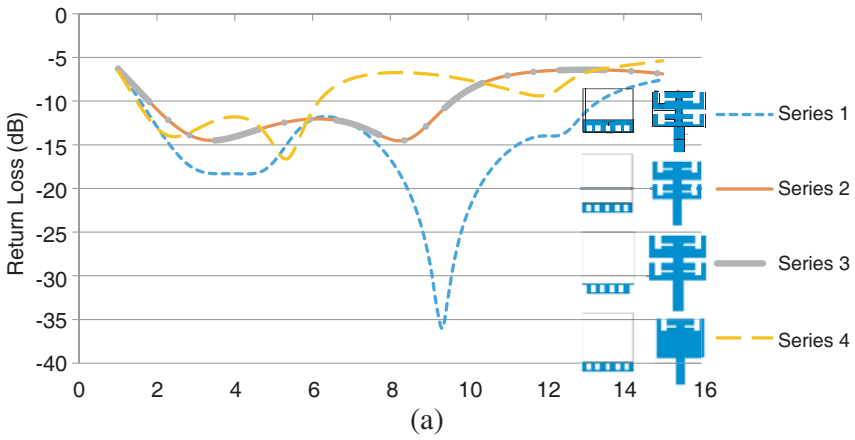

(a)

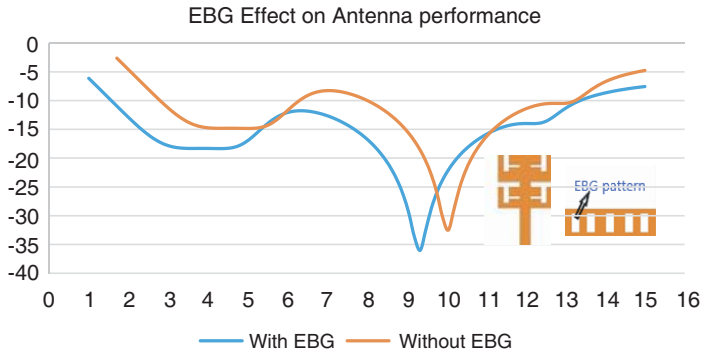

(b)

Figure 7. Variation of S_{11} parameters, (a) design evolution, (b) EBG characteristics.

modified fractal trident geometry is analysed on different combinations of EBG structures on the ground surface. After successive iterations, antenna series 1 exhibits very high performance for simulated return loss characteristics in operating range of 1.55–13.33 GHz. The complete comparisons among various designs are represented by antenna series 1–4 with respect to antenna evolutions. The phenomenon, behind this, is the effect of capacitive loading in parallel combinations. The ground deformations are

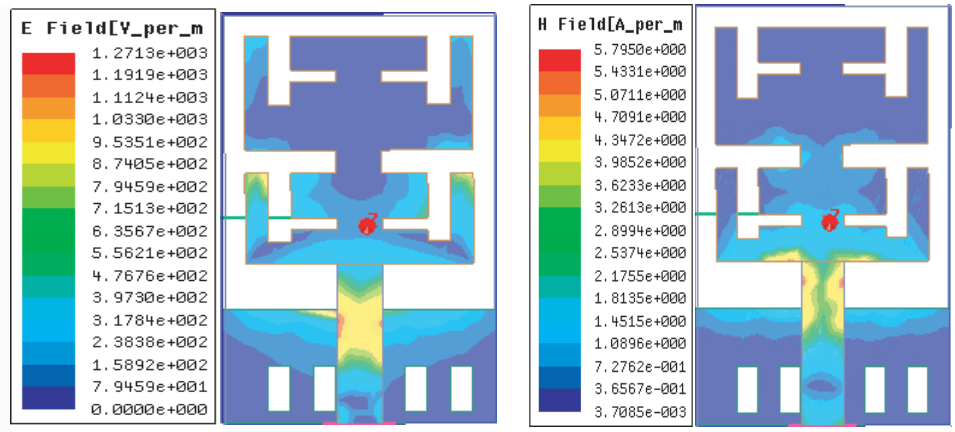

(a) (b)

Figure 8. (a) Electric and (b) magnetic field distribution.

made by truncation of vertical dimensions of rectangular ground. However, rectangular slots represent the effect of EBG structure in pre-optimized ground geometries through DGS. The straight comparison is shown in Figure 7(b), to show the effect on inclusion of pattern in ground geometry. From the comparison, it is validated that the antenna geometry possesses better match of electrical impedance of antenna geometry over complete operating range, and hence, the antenna is able to exhibit radiation on lower range of frequency without any enhancement in the physical dimension.

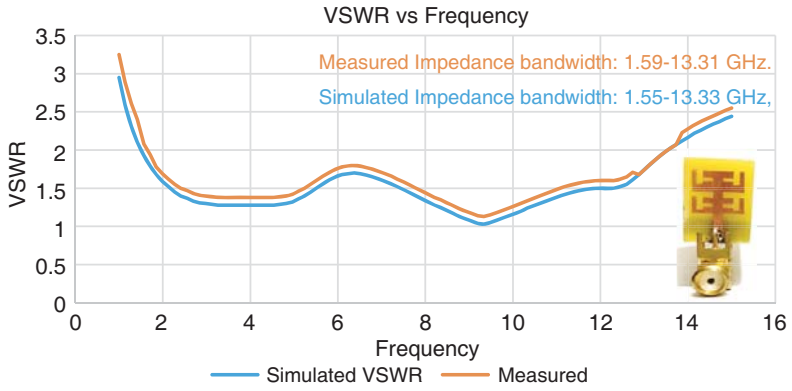

Figure 9. Simulated and measured variation of VSWR.

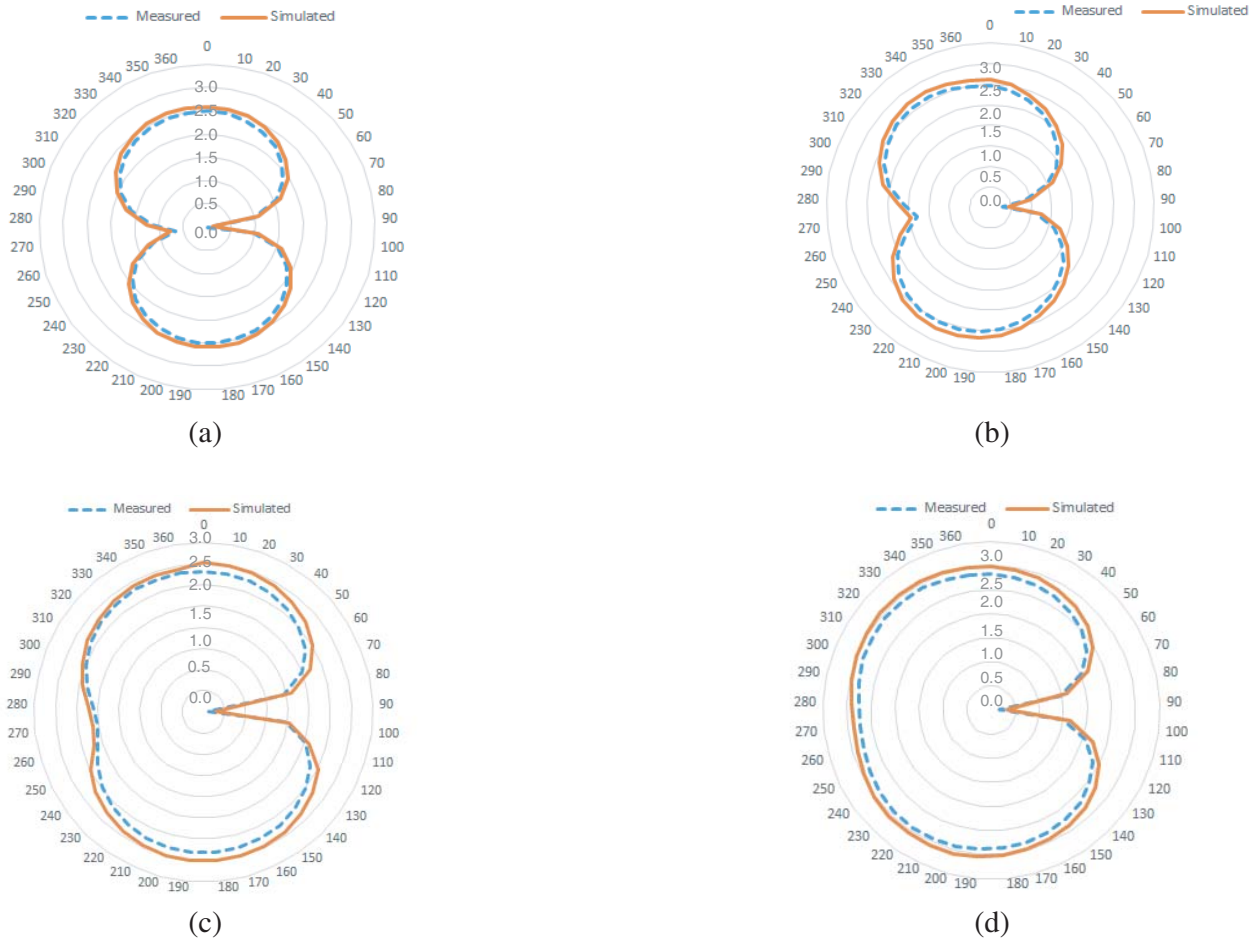

Figure 10. Simulated E-plane radiation patterns (a) at 2.5 GHz, (b) at 5 GHz, (c) 7.5 GHz, (d) 10 GHz.

This enhances the reactance to make feed current lead forward with respect to voltages across the patch edges. The field distribution is shown in Figure 8. The electric and magnetic field distributions are shown for the field expansion from the centre of the patch to the edges. This field extends in transverse

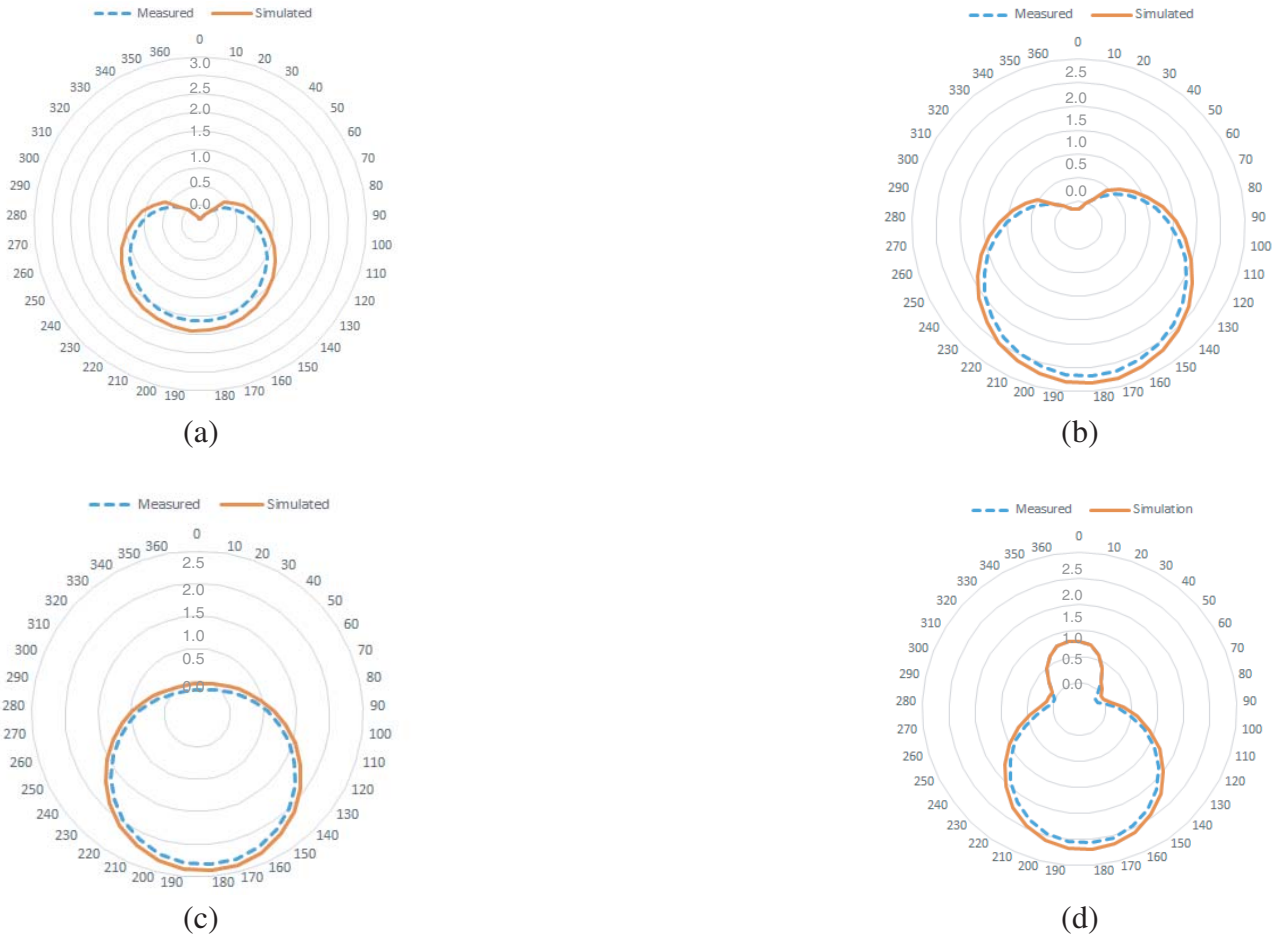

Figure 11. Simulated H-plane radiation patterns (a) at 2.5 GHz, (b) 5 GHz, (c) 7.5 GHz, (d) 10 GHz.

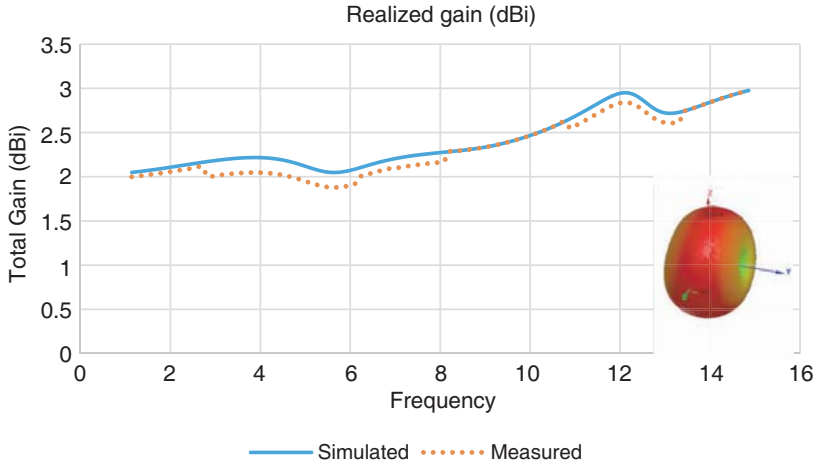

Figure 12. Gain of the antenna over operating frequency.

modes in the far-field region of the antenna. Figure 9 shows the design validation of the fabricated prototype using Rohde & Schwarz ZVA 40 vector network analyser. The results are promising between measured and simulated VSWR values as indicated in Figure 9 under experimental limitations. Hence, the antenna is quite suitable for various IoT applications. The E & H plane radiation patterns for different frequency segments are found consistent as shown in Figures 10 & 11. This helps the antenna to sustain a stable radiation pattern for complete bandwidth and therefore, feasible as transceivers. Therefore, the antenna structure is highly matched at the wider side of the patch geometry, while the fractal limbs resonate at the comparatively high edge of frequency.

The measured results of the proposed antenna have a −10 dB impedance bandwidth from 1.59 to 13.31 GHz, covering the WLAN (2.4 GHz), WiMAX (2.5 GHz), and complete UWB (3.1–10.6 GHz). The simulated and measured normalized far-field radiation patterns in E-plane and H-plane at frequencies 2.5, 5, 7.5, and 10 GHz are recorded.

For design validation, the total antenna gain is observed over the entire band of operating frequency and lies between 2 and 3 dBi as shown in Figure 12. The IoT devices require predefined polarization characteristics of antenna devices. RFID tags may be circularly polarized or linearly polarized, depending upon the plane of installation. To avoid the plane of symmetry, RHCP, LHCP, or both may be preferred during installation of two-way communication in IoT embedded systems on network layer. Figure 13 shows LHCP with satisfactory 3 dB axial ratio bandwidth over the entire operating range. The proposed antenna has edge in-depth digging of orthogonal slots geometry at two vertical sides and twice on upper horizontal edge. This enables the antenna to generate two orthogonal modes for circular polarization. The operating principle to obtain the circular polarization is adopted from the split phase phenomenon of the trident symmetry. Specifically, the current fed from the patch strip is distributed in two phases at the two truncated trident edges, which has been able to provide a quarter shift to the phase current, and hence the orthogonal modes causes CP. In the same sequence, the antenna has been observed for its main beam direction. Figure 14 shows that the total gain of the antenna in the E plane remains almost consistent for bidirectional pattern in 0 and 180 degree positions and shows almost nulls at 90 and 270 degrees. Thus, the proposed antenna also exhibits sustainable polarization properties, which makes it conveniently usable for IoT based devices. After successive iterations and experimental analysis of the antenna, the proposed design is suitable for multipurpose wireless applications of modern IoT technology. In this reference, the novelty of the antenna is validated through comparison with other previously reported standards in UWB antenna designs as shown in Table 3.

Therefore, on behalf of comparative study, the antenna is highly feasible for UWB applications. In addition to this, it offers satisfactory radiating characteristics in the lower band of 1.59–13.31 GHz for multiple IoT applications. This proposed design is very compact in size and compatible with many wireless systems in its broad operating range.

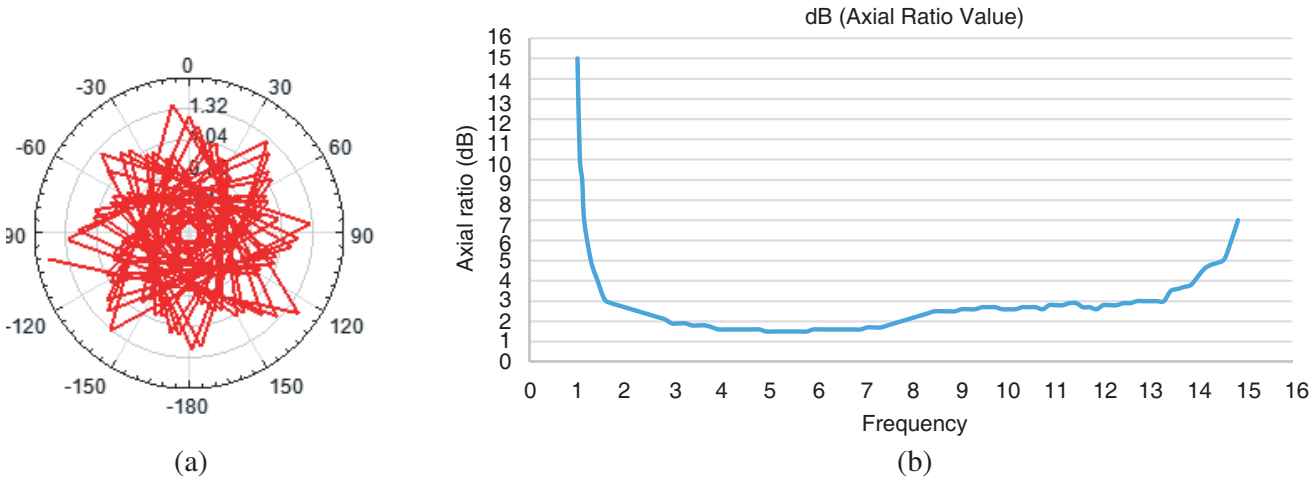

(a) (b)

Figure 13. (a) LHCP over the entire operating frequency sweep, (b) axial ratio.

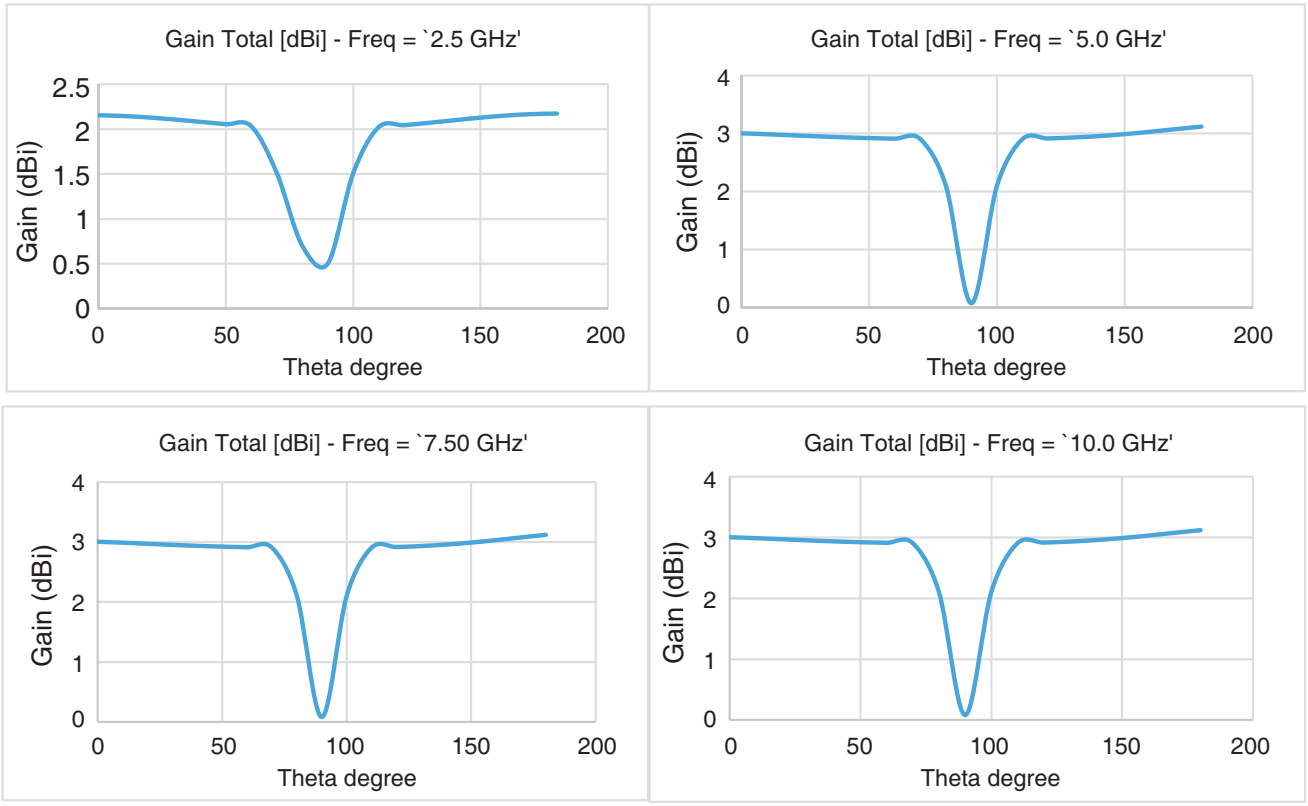

Figure 14. Main beam direction at 2.5, 5, 7.5 and 10 GHz frequency.

Table 3. Design validation.

Parameter/ Ref.	Band (GHz.)	Material	Dimension (mm)	Remark
[25]	2.94–22.2	FR4	25 × 17	The antenna operates only in UWB region
[26]	2.5–12	FR4	48 × 48	Notched band at 5.5 GHz at large structure
[27]	3.04–10.87	FR4	20 × 20	Band Rejections
[28]	5–15	FR4	11 × 15	Notched band 6.7–7.1-GHz more shifted to upper bands
[29]	3.04–10.87	FR4	20 × 20	Band Rejections at 5.03 to 5.94 GHz
[30]	2.5–12	FR4	48 × 48	Enlarged size with rejection at 5.5 GHz
[31]	3.6–11.6	FR4	30 × 34	Complete UWB but high in size
[32]	5–15	FR4	11 × 15	Notched band 6.7–7.1-GHz missing lower edge frequency
[33]	3.1–16	FR4	22 × 26	Only UWB, even on larger patch dimension
Proposed	**1.59–13.31**	**FR4**	**12 × 18**	**UWB, Bluetooth, GPS etc. with lower frequency edging at significant miniaturized structure**

4. CONCLUSION

To fulfill the requirement of a wireless IOT based home automation and smart industry, an advanced, efficient, high gain, and broadband antenna is needed. The antenna proposed in this paper is highly compact and exhibits a very large bandwidth with high gain and good radiation characteristics. The antenna is based on the smart use of a slotted structure in antenna design. The finalized antenna is trident in shape, exhibiting fractal properties with DGS and EBG effects. The antenna is found suitable for IoT based wireless application between the ranges of 1.59 and 13.31 GHz frequencies. The antenna has high gain characteristic to make use of it for real-time applications. The simulated and measured results are in a good compromise.

REFERENCES

1. Nosrati, M. and N. Tavassolian, "Miniaturized circularly polarized square slot antenna with enhanced axial-ratio bandwidth using an antipodal Y-strip," *IEEE Antennas Wireless Propag. Lett.*, Vol. 16, No. 8, 17–20, 2016.
2. Jhajharia, T., V. Tiwari, D. Bhatnagar, D. Yadav, and S. Rawat, "A dual-band CP dual-orthogonal arms monopole antenna with slanting edge DGS for C-band wireless applications," *Int. J. Electron. Commun.*, Vol. 84, 251–258, 2018.
3. Chen, N. Z. N., "Multipatches multilayered UWB microstrip antenna," *IET Microwave Antennas Propog.*, Vol. 3, 379–386, 2009.
4. Toh, W. K., Z. N. Chen, X. Qing, and T. S. P. See, "A planar UWB diversity antenna," *IEEE Trans. Antennas Propag.*, Vol. 57, 3467–3473, 2009.
5. Azim, R., M. T. Islam, and N. Misran, "Compact tapered-shape slot antenna for UWB applications," *IEEE Antennas Wireless Propag. Lett.*, Vol. 10, 1190–1193, 2011.
6. Piyare, R. and M. Tazil, "Bluetooth based home automation system using cell phone," *IEEE 15th International Symposium on Consumer Electronics*, 2011.
7. Kelly, S. D. T., N. K. Suryadevara, and S. C. Mukhopadhyay, "Towards the implementation of IoT for environmental condition monitoring in homes," *IEEE Sensors Journal*, Vol. 13, 3846–3853, 2013.
8. Piyare, R., "Internet of things: Ubiquitous home control and monitoring system using android based smart phone," *International Journal of Internet of Things*, 2013.
9. Vasylchenko, A., Y. Schols, W. De Raedt, and G. A. E. Vandenbosch, "Quality assessment of computational techniques and software tools for planar-antenna analysis," *IEEE Antennas and Propagation Magazine*, Vol. 51, No. 1, 23–38, 2009, ISSN: 1045-9243.
10. Pham, N. T., G. Lee, and F. De Flaviis, "Minimized dual-band coupled line meander antenna for system-in-package applications," *IEEE Antennas and Propagation Society International Symposium*, Vol. 2, 1451–1454, Jun. 2004.
11. Kim, Y. M., "Ultra wide band (UWB) technology and applications," Technical Report, NEST Group, The Ohio State University, Jul. 2003.
12. Cheng, Z. N., et al., "Planar antennas," *IEEE Microwave Magazine*, Vol. 7, No. 1, 63–73, 2006.
13. Lee, Y. C., W. J. Huang, and J. S. Sun, "A study of printed monopole antenna for ultra wideband systems," *International Symposium on Antennas and Propagation — ISAP*, 1–4, 2006.
14. Ray, K. P. and Y. Ranga, "Ultrawideband printed elliptical monopole antennas," *IEEE Trans. Antennas Propag.*, Vol. 55, No. 4, 1189–1192, Apr. 2007.
15. Chen, Z. N., T. S. P. See, and X. Qing, "Small printed ultra wideband antenna with reduced ground plane effect," *IEEE Trans. Antennas Propag.*, Vol. 55, No. 2, 383–388, Feb. 2007.
16. John, M. and M. J. Ammann, "Wideband printed monopole design using a genetic algorithm," *IEEE Antennas Wireless Propag. Lett.*, Vol. 6, 447–449, 2007.
17. Ray, K. P., "Design aspects of printed monopole antennas for ultra-wide band applications," *International Journal of Antennas and Propagation*, 1–8, 2008.

18. Radiom, S., H. Aliakbarian, G. A. E. Vandenbosch, and G. G. E. Gielen, "An effective technique for symmetric planar monopole antenna miniaturization," *IEEE Trans. Antennas Propag.*, Vol. 57, No. 10, 2989–2996, Oct. 2009.
19. Muge, F., T. Tigrek, A. Hizar, L. E. Lager, and L. P. Ligthart, "On the operating principles of UWB, CPW-fed printed antennas," *IEEE Antennas and Propagation Magazine*, Vol. 52, No. 3, 46–50, Jun. 2010.
20. Ebrahimi, E., J. R. Kelly, and P. S. Hall, "Integrated wide-narrowband antenna for multi-standard radio," *IEEE Trans. Antennas Propag.*, Vol. 59, No. 7, 2628–2635, Jul. 2011.
21. Gupta, S. D. and M. C. Srivastava, "Multilayer microstrip antenna quality factor optimization for bandwidth enhancement," *Journal of Engineering Science and Technology*, Vol. 7, No. 6, 756–773, Dec. 2012.
22. Fereidoony, F., S. Chamaani, and S. A. Mirtaheri, "Systematic design of UWB monopole antennas with stable omnidirectional radiation pattern," *IEEE Antennas Wireless Propag. Lett.*, Vol. 11, 752–755, 2012.
23. Guo, Z., H. Tian, X. Wang, Q. Luo, and Y. Ji, "Bandwidth enhancement of monopole UWB antenna with new slots and EBG structures," *IEEE Antennas Wireless Propag. Lett.*, Vol. 12, 1550–1553, 2013.
24. Gupta, K. C., R. Garg, I. Bhal, and P. Bhartia, *Microstrip Lines and Slot Lines*, 2nd Edition, Artech House, Inc., Norwood, MA, 1996.
25. Tiwaria, R. N., P. Singh, and B. K. Kanaujia, "A modified microstrip line fed compact UWB antenna for WiMAX/ISM/WLAN and wireless communications," *AEU — International Journal of Electronics and Communications*, Vol. 104, 58–65, May 2019.
26. Gao, P., S. He, X. Wei, Z. Xu, N. Wang, and Y. Zheng, "Compact printed UWB diversity slot antenna with 5.5-GHz band-notched characteristics," *IEEE Antennas Wireless Propag. Lett.*, Vol. 13, 376–379, Feb. 2014.
27. Ojaroudi, M. and N. Ojaroudi, "Ultra-wideband small rectangular slot antenna with variable band-stop function," *IEEE Trans. Antennas Propag.*, Vol. 62, No. 1, 490–494, Jan. 2014.
28. Nguyen, D. T., D. H. Lee, and H. C. Park, "Very compact printed triple band-notched UWB antenna with quarter-wavelength slots," *IEEE Antennas Wireless Propag. Lett.*, Vol. 11, 411–414, Apr. 2012.
29. Ojaroudi, M. and N. Ojaroudi, "Ultra-wideband small rectangular slot antenna with variable band-stop function," *IEEE Trans. Antennas Propag.*, Vol. 62, No. 1, 490–494, Jan. 2014.
30. Gao, P., S. He, X. Wei, Z. Xu, N. Wang, and Y. Zheng, "Compact printed UWB diversity slot antenna with 5.5-GHz band-notched characteristics," *IEEE Antennas Wireless Propag. Lett.*, Vol. 13, 376–379, Feb. 2014.
31. Wu, J., Z. Zhao, Z. Nie, and Q. H. Liu, "Bandwidth enhancement of a planar printed quasi-yagi antenna with size reduction," *IEEE Trans. Antennas Propag.*, Vol. 62, No. 1, 463–467, Jan. 2014.
32. Ellis, M. S., Z. Zhao, J. Wu, Z. Nie, and Q. H. Liu, "A novel miniature band-notched wing-shaped monopole ultra wide-band antenna," *IEEE Antennas Wireless Propag. Lett.*, Vol. 12, 1614–1617, 2013.
33. Khan, Z., A. Razzaq, J. Iqbal, A. Qamar, and M. Zubair, "Double circular ring compact antenna for ultra-wideband applications," *IET Microwaves, Antennas & Propagation*, Vol. 12, No. 13, 2094–2097, 2018.